Mirror states in $A = 15$ from 60-MeV ^{6}Li-induced reactions on ^{12}C

H. G. Bingham,† M. L. Halbert, D. C. Hensley, and E. Newman
*Oak Ridge National Laboratory, Oak Ridge, Tennessee 37830**

K. W. Kemper and L. A. Charlton
Department of Physics, The Florida State University, Tallahassee, Florida 32306‡

(Received 11 February 1975)

Analog pairs of states have been observed simultaneously with counter telescopes by using the ^{12}C(^{6}Li, t) and ^{12}C(^{6}Li,^{3}He) reactions for $E(^6\text{Li}) = 60$ MeV at excitation energies of 10.45-10.73, 12.84-13.15, and 15.05-15.49 MeV in ^{15}O-^{15}N, respectively. Magnetic spectrograph data for the ^{12}C(^{6}Li, t)^{15}O reaction having an energy resolution of 50 keV versus the 200 keV resolution of the counter systems show that single states are being strongly excited at 10.45, 12.84, and 15.05 MeV in ^{15}O. Elastic and inelastic scattering data have also been taken in the angular range from 10 to 120° c.m. with $\Delta\theta \approx 2°$. Optical model parameters were extracted from the elastic scattering data, and quadrupole deformation lengths were obtained from a coupled-channels analysis of the inelastic scattering data to the 2^+, 4.43-MeV state in ^{12}C. Exact finite-range distorted-wave Born-approximation calculations for the transfer reactions yield a range of L transfers for each of the analog states which are consistent with the assumption that these states have spins $J_f \geq \frac{9}{2}$.

[NUCLEAR REACTIONS ^{12}C(^{6}Li, ^{6}Li$_{0,1,2}$), (^{6}Li, ^{3}He-t) $E = 60$ MeV; measured $\sigma(\theta)$; deduced optical model parameters; coupled-channels calculations, deduced β_2; identified mirror states in ^{15}O-^{15}N; deduced range of L transfers for each mirror state from finite range DWBA analyses.]

I. INTRODUCTION

A growing body of data on the (^{6}Li, ^{3}He) and (^{6}Li, t) reactions on low-A self-conjugate nuclei has shown that these reactions are very selective, tend to favor the population of high spin states, and provide a means for identifying analog states in the residual mirror nuclei. The studies[1-3] carried out at 18 and 24 MeV on targets of ^{10}B, ^{14}N, and ^{16}O suffered from two complications; compound-nucleus effects may have been important, and barrier inhibition in the exit channel caused an uncertainty in the relative strenghts of the high-spin members of a particular configuration. A 36-MeV study of the ^{16}O(^{6}Li, t) reaction[4] indicated that both these difficulties could be eliminated with higher beam energy and that selective population continues up to much higher excitation energies than previously observed. Preliminary surveys with beams of 60-MeV ^{6}Li^{++} from the Oak Ridge isochronous cyclotron (ORIC) revealed that the ^{3}He and triton spectra from carbon targets showed remarkably strong and highly selective excitation of levels up to nearly 20 MeV in both ^{15}N and ^{15}O.

The present work reports the results of a study of ^{6}Li-induced three particle transfer reactions on ^{12}C. The experimental results presented consist of angular distributions for the ^{12}C(^{6}Li, ^{3}He-t) reactions obtained with counter telescopes, higher resolution triton spectra taken at forward angles with a magnetic spectrograph and ^{6}Li + ^{12}C elastic and inelastic scattering angular distributions. The elastic scattering data were analyzed in terms of the optical model, and the inelastic scattering data were analyzed with the coupled-channels method. Limiting values for the transferred angular momenta to observed analog states have been deduced for the (^{6}Li, ^{3}He-t) data on the basis of exact finite-range distorted-wave Born-approximation (FRDWBA) calculations.

II. EXPERIMENTAL METHOD

The ^{6}Li^{++} beam was produced copiously by a special adaptation of the standard ORIC cold-cathode heavy-ion source.[5] A half-cylindrical carbon shell was filled with ^{6}LiF powder and heated with a torch to fuse the powder into a glassy deposit. The shell was inserted into the ion source tube and an arc was struck with neon gas. Beam intensities registered in the Faraday cup were often as high as 200 nA.

To measure angular distributions for the three particle transfer reactions, bombardments were carried out in a 76-cm diam scattering chamber

using a 59.7-MeV beam of $^6Li^{++}$ prepared with a resolution of about ±0.05 MeV by means of an analyzing magnet. Two independent silicon surface-barrier counter telescopes were used simultaneously. The first, used for laboratory angles from 10 to 32.5°, consisted of three counters, a 403-μm ΔE counter and two 3-mm detectors connected together to form a 6-mm E detector. The other telescope, used from 40 to 60°, was composed of a 277-μm ΔE counter and a 5-mm E counter. The energy resolution was about 200 keV for both telescopes, and the over-all angular resolution (including spot size and beam divergence) was about 0.7°. The solid angle for each telescope was measured by means of an α source of known strength placed at the target position.

The ΔE and sum-E signals ($E + \Delta E$ analog sum) for each telescope were recorded by means of a multiplexed 8192-channel analog-to-digital converter (ADC) coupled to an on-line computer.[6] An associative-memory program[7] was used for temporary storage in the core memory. After a buffer was filled, an alternate buffer was automatically initialized and the data in the first buffer transferred to disk storage, with a full ΔE, sum-E array being reconstructed on the disk[7] for each telescope. These arrays could be plotted as contour maps on the line printer or the interactive storage-scope display. The events due to each type of particle were selected and projected onto the sum-E axis to produce one-dimensional energy spectra, which could then be analyzed on the display unit by means of a peak-fitting program.

The target was natural carbon (98.9% ^{12}C) of thickness 165 ± 20 μg/cm^2, as determined by energy-loss measurements with an α source. Cross sections were calculated from the known geometry, target thickness, and integrated beam current in the Faraday cup (operated with −300 V on the suppressor). The ^6Li reaching the cup was assumed to be fully stripped by its passage through the target. The uncertainty in the cross sections is ±15%, due mainly to the target thickness. Of course, the relative ^3He and t cross sections at any given angle are not subject to these systematic uncertainties since the spectra were obtained simultaneously.

To better determine the number of states contributing to a given peak obtained with the counter telescopes, higher resolution ($^6Li, t$) data were obtained with the ORIC broad-range spectrograph, based on the Copenhagen design,[8] as described by Ball.[9] Nuclear emulsion plates were exposed at 5, 10, and 15° lab. Absorbers were placed in front of each plate to slow down the tritons. Three plates, each 252 mm long, were placed end to end in order to record the wide range of triton energies encountered in this experiment.

The beam energy was 60.0 ± 0.1 MeV, with an estimated spread of about ±0.04 MeV. A natural carbon target of nominal thickness 40 μg/cm^2 was used; the actual thickness was not measured.

The elastic and inelastic scattering data were obtained in the 76 cm scattering chamber when it was located on a low-resolution beam line. Although the beam was passed through a bending magnet, it was focused on the target nondispersively by demanding an intermediate crossover halfway through this magnet.[10] From similar studies with other beams, the energy resolution is estimated to have been ±0.2 or 0.3 MeV. Before the scattering measurements, the beam was switched to the high-resolution line including the calibrated analyzing magnet to determine its ener-

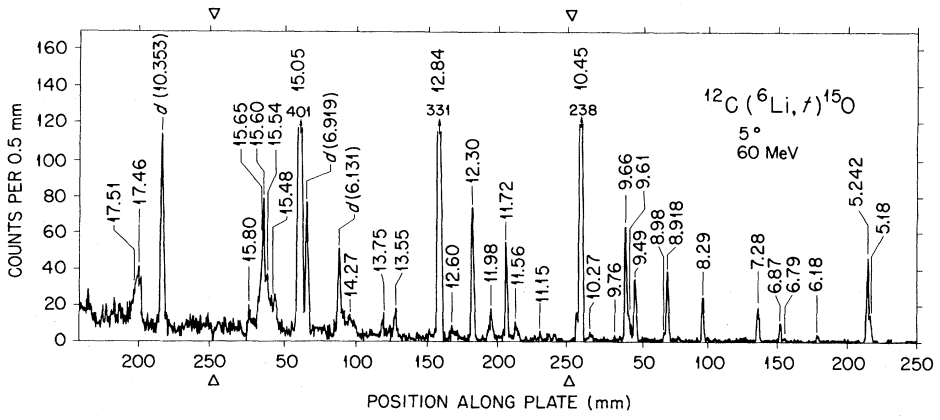

FIG. 1. Triton spectrum at a lab angle of 5° from the $^{12}C(^6Li, t)^{15}O$ reaction taken in a magnetic spectrograph for a beam energy of 60 MeV. The triangles indicate the boundaries between adjacent plates. The numbers refer to excitation energies in ^{15}O deduced from this spectrum and similar data at 10 and 15°. The three peaks labeled d are due to deuterons corresponding to the known ^{16}O excitation energies shown in parentheses.

TABLE I. Energy levels of ^{15}O. The excitation energies in the second and third columns are from the present experiment. The energies in the second column are to ±5 keV up to 11 MeV, ±10 keV up to 16 MeV, and ±20 keV above this. The c.m. cross sections from the 10° (lab) telescope data are shown in the fourth column.

Excitation energy				
Previously known [a] (MeV ± keV)		Spectrograph (MeV)	Telescope (MeV)	$\sigma_{c.m.}$ (10°) (mb/sr) (±15 %)
5.181	±5	5.180	5.24	0.154
5.241 51	±0.52	5.242		
6.177	±3	6.179		
6.788	±4	6.790		
6.859	±1	6.865	6.92	0.048
7.2760	±0.6	7.275	7.29	0.091
8.2833	±1.5	8.285	8.33	0.081
8.9180	±1.4	8.918		
8.9781	±1.6	8.978	8.95	0.106
9.483	±3	9.485		
9.606	±1.8	9.610		
			9.63	0.310
9.660	±4	9.658		
9.72	±50	9.76		
10.278	±8	10.27		
10.46	±10	10.45	10.50	0.541
		11.145		
11.56, 11.57	±15	11.56		
11.71	±15	11.72	11.73	0.219
11.98	±15	11.98		
		12.295		
			12.38	0.175
		12.60		
12.82		12.835	12.88	0.928
		13.55		
			13.63	0.105
		13.75		
14.27	±40	14.27	14.27	0.231
		15.05	15.05	1.361
		15.48		
		15.54		
		15.60	15.61	0.744
		15.65		
		15.80		
		17.46		
17.50	±50		17.49	0.208
		17.51		

[a] See Ref. 12.

gy; the result was 59.8 ± 0.2 MeV.

The detector was a position-sensitive silicon detector fitted with an eight-slit collimator. Each slit was 0.32 cm wide and subtended 1.0° lab. The slits were 2.0° apart, so that a 14° interval was covered with one setting. At small angles, the assembly was moved to intermediate settings to obtain measurements at 1° intervals.

The multiplexed-ADC system[6] was used to digitize the $P \times E$ and E signals supplied by the detector. The computer divided the first of these by the second to obtain the position descriptor P. The data array parametrized by P and E was then processed by the same programs[7] mentioned above.

The solid angle of each slit was determined by means of the calibrated α source at the target position. The 165-μg/cm^2 target was used and absolute cross sections were again calculated from the integrated beam, known target thickness, and solid angle, with an estimated accuracy of ±15%. The relative shape is much more accurate than this since the data were obtained for eight angles at once. When the detector was moved to cover a new set of angles, it was always positioned to re-

peat several angles from some preceding run; the cross sections from such overlapping data agreed within a few percent. The elastic cross sections obtained in the present work are 30–35% higher than those obtained earlier by Ollerhead, Chasman, and Bromley[11] for 63 MeV ^{6}Li from ^{12}C but are within the combined experimental errors from the two experiments.

III. EXPERIMENTAL RESULTS

Figure 1 shows the triton spectrum obtained with the spectrograph at 5°. The energy scale for each of the three plates was established by reference to well-known levels[12,13] because experimental uncertainties in the plate positions precluded an absolute calibration. For the first plate, showing groups in ^{15}O below 11 MeV excitation, the 5.242- and 8.918-MeV levels[12] were taken as the basis. The energies of the other 12 accurately known levels[12] on this plate were then found to be correct within 8 keV. Two deuteron groups, corresponding to the second and third excited states[13] of ^{16}O, appeared on the second plate and were used to establish its energy scale. Five of the triton groups on this plate correspond to ^{15}O excitation energies within about 10 keV of known levels[12] at 11.56, 11.71, 11.98, 12.82, and 14.27 MeV. For calibrating the third plate, the strong deuteron group was assumed to be from the 10.353-MeV level[13] of ^{16}O; an error of 1 keV in this energy would shift the ^{15}O energies by 0.63 keV.

Similar analyses of the plates at 10 and 15° resulted in excitation energies that were generally consistent with the 5° results within 10 keV; the worst discrepancies did not exceed 25 keV. Table I lists the excitation energies deduced from combining these results for all groups appearing clearly for at least two of the three angles. In many cases, for example the strong 15.05-MeV group, no level tabulated in Ref. 12 can be positively identified with those seen here.

Figure 2 shows the ^{3}He and triton spectra taken simultaneously with the counter telescope at 10°. The two spectra are remarkably similar, both in absolute yields of the prominent peaks and in their relative intensities. The strong selectivity at high excitation should also be noted: Only a few of the many states known to exist are excited in this reaction. The relative strengths of the prominent peaks agree very well with the yields for states at similar excitation energies from the

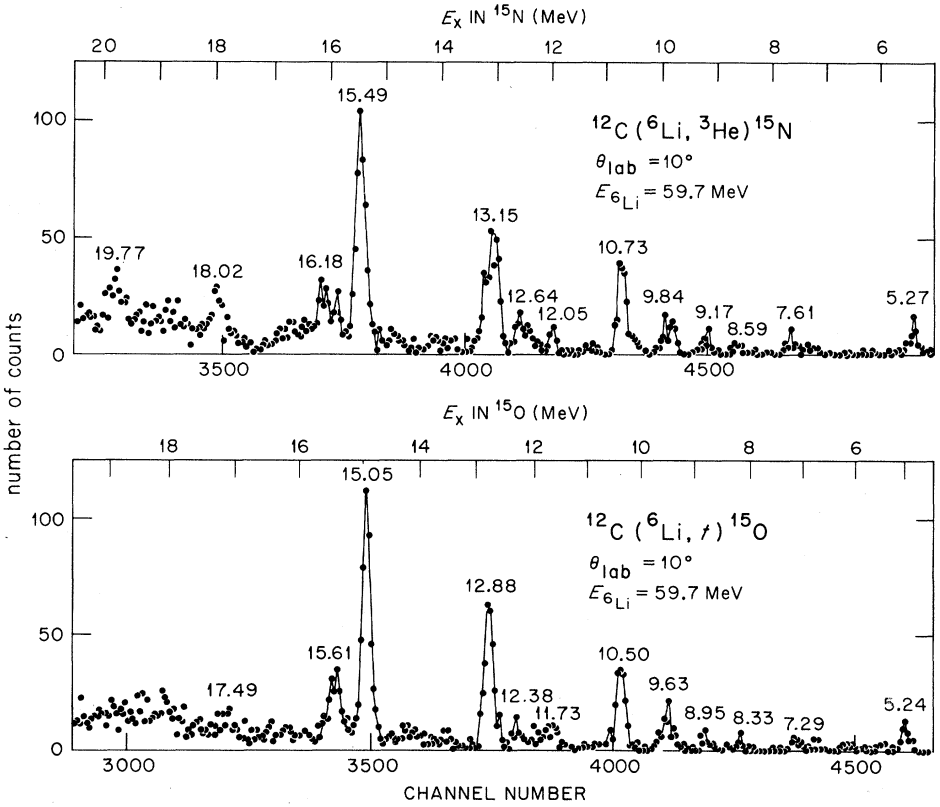

FIG. 2. Energy spectra from the ^{12}C(^{6}Li, ^{3}He) and ^{12}C(^{6}Li, t) reactions taken simultaneously. The energy scales were inferred from the energies of known low-lying states.

TABLE II. Energy levels of ^{15}N. The excitation energies are accurate to about ±60 keV. The c.m. cross sections are from the spectrum at 10° lab.

Excitation energy (MeV)	$\sigma_{c.m.}$ (10°) (mb/sr) (±15%)
5.27	0.177
7.24	0.065
7.61	0.106
8.59	0.064
9.17	0.120
9.84	0.269
10.73	0.597
12.05	0.130
12.36	0.158
12.64	0.214
13.15	1.078
15.49	1.540
15.88	0.282
16.18	0.473
16.41	0.206
16.74	0.274
18.02	0.540
19.77	0.795

^{12}C(^{10}B, ^{7}Li) and ^{12}C(^{10}B, ^{7}Be) reactions.[14] The cross sections for the ^{6}Li-induced reactions are about 5 times larger than for the ^{10}B reactions.

The triton energy scale in Fig. 2 was obtained independently of the spectrograph results by reference to the known 5.242- and 9.660-MeV levels[12]; the energy assignments are given in Table I. The energies of the prominent peaks agree with the spectrograph results within 10 keV.

The energy scale for the ^{3}He was found to be slightly different (0.4%), probably because of a slightly imperfect gain adjustment of the signals combined in the $E+\Delta E$ summation. The calibration used in Fig. 2 is based on the well-known 5.27-MeV level[12] of ^{15}N. It was found to work well for the four most energetic α groups from ^{12}C(^{6}Li, α)^{14}N, which have approximately the same ΔE as the ^{3}He but a much higher sum E. The ^{15}N excitation energies deduced from this calibration agree with known low-lying levels[12] of ^{15}N within about 60 keV, as indicated in Table II. The ^{15}N energies inferred from the ^{3}He spectra at 12.5 and 15° are consistent with the 10° results within 60 keV. Tables I and II list the 10°(13.4–14.2° c.m.) cross sections for all groups identified in the tele-

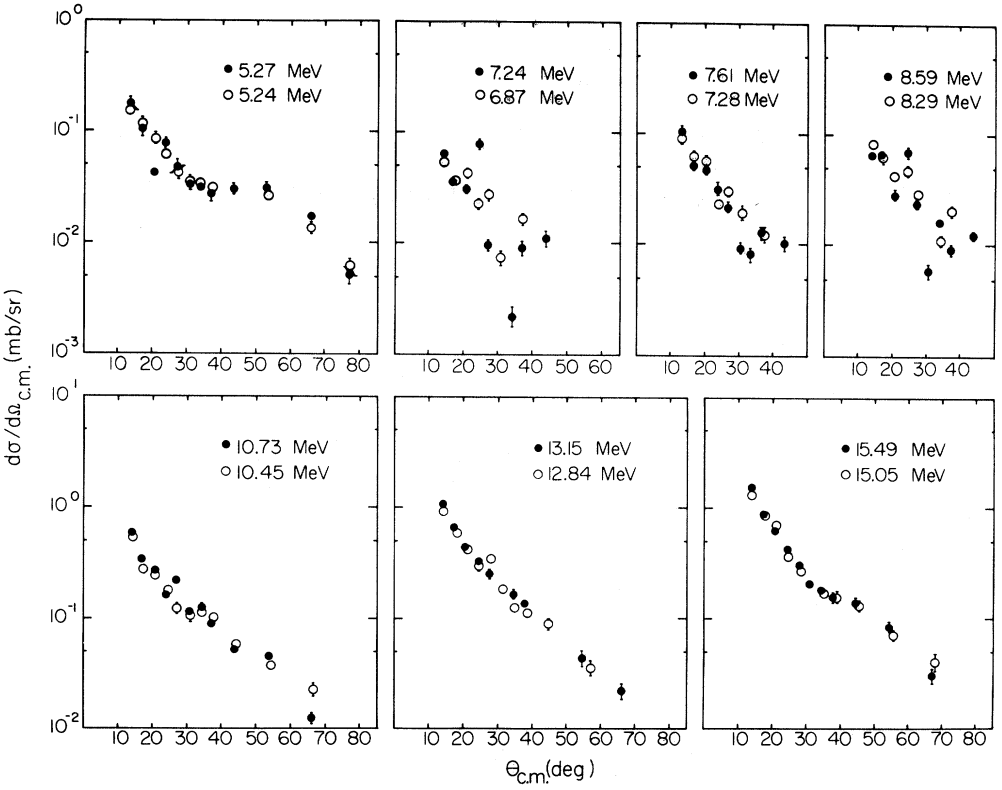

FIG. 3. Angular distributions for the reactions ^{12}C(^{6}Li, ^{3}He)^{15}N (closed circles) and ^{12}C(^{6}Li, t)^{15}O (open circles) leading to mirror states in ^{15}N and ^{15}O. Note that the cross section scale for the top row of low-lying states is reduced by a factor of 10 from the bottom row of high-lying states.

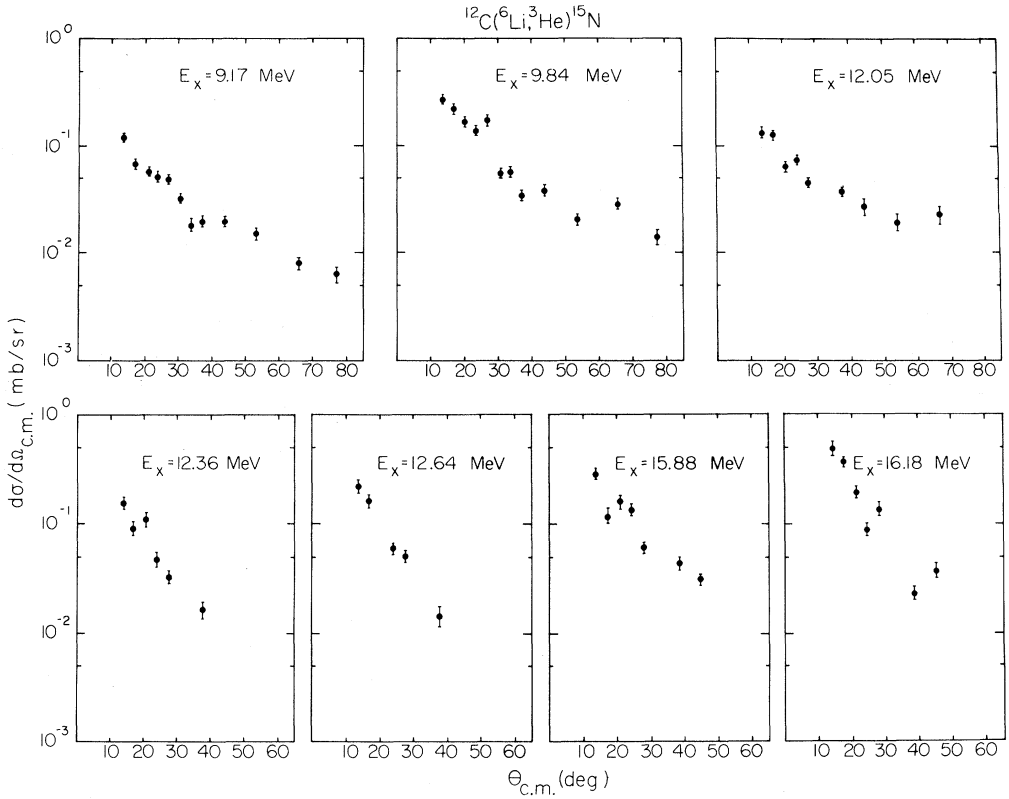

FIG. 4. Angular distributions for the reaction $^{12}C(^{6}Li, ^{3}He)$ to states or groups of states in ^{15}N for which corresponding analog state assignments in ^{15}O could note be made.

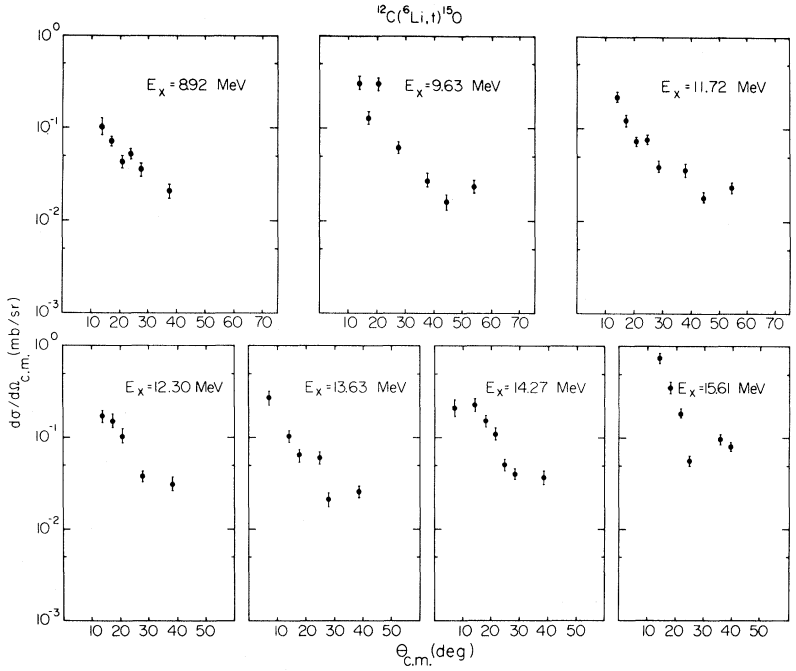

FIG. 5. Angular distributions for the reaction $^{12}C(^{6}Li, t)$ to states or groups of states in ^{15}O for which corresponding analog states in ^{15}N could not be identified.

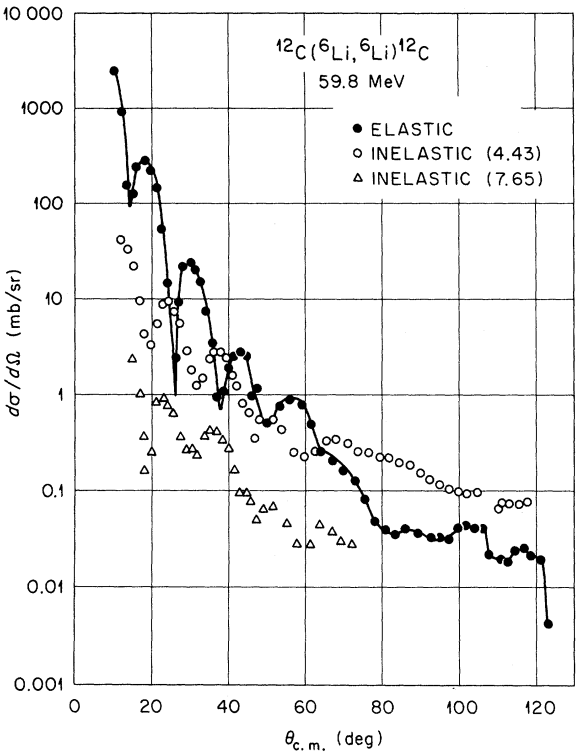

FIG. 6. Elastic scattering data for ^{6}Li + ^{12}C at $E_{^6\mathrm{Li}}$ = 59.8 MeV. Also shown is the inelastic scattering data to the 2^+, 4.43 MeV and 0^+, 7.65 MeV states in ^{12}C. The solid curve is only to guide the eye.

scope data. The differential cross sections deduced from the telescope data are shown in Figs. 3–5. The groups above 16 MeV could not be followed out to large angles. The errors shown in the figures represent the statistical counting errors.

Figure 6 shows the cross sections for the elastic scattering and inelastic scattering to the 4.43- and 7.65-MeV levels of ^{12}C. Higher states of ^{12}C were excited, but cross sections were not obtained because of background problems. Little or no evidence was found for excitation of the 3.56-MeV $T=1$ level of ^{6}Li; the other excited states of ^{6}Li are unstable and would disintegrate before reaching the detector.

IV. ANALYSIS AND DISCUSSION

A. Elastic and inelastic scattering

Previous optical model analyses of ^{6}Li elastic scattering for bombarding energies in the range 20–36 MeV have shown that the optical model is able to describe the data even though ^{6}Li is a relatively complex projectile. To determine whether this conclusion also holds at the higher energy used in this work, as well as to provide optical model parameters for use in subsequent distorted-wave Born-approximation (DWBA) analyses of the transfer reaction data, optical model calculations were done with the program JIB.[15] The standard form of the optical potential with a volume imaginary potential was used. The initial calculations were carried out with parameters taken from the literature.[2,16,17] A spin-orbit potential was not included in any of the calculations because of the absence of polarization data. The specific parameter sets used in the calculations were the sets with $U=173$ MeV obtained from analyses of 28- and 34-MeV data in Refs. 16 and 17 and a parameter set with $U=159$ and $W=7$ MeV which was used in DWBA calculations that were successful in describing the shape of ^{16}O(^{6}Li, ^{3}He-t)^{19}F angular distributions at a bombarding energy of 24 MeV.[2] The six parameters were varied in pairs in the sequence (a_r, r_i), (r_r, a_i), and (U, W) until minimum χ^2 was attained. The best fit to the data resulting from these searches is shown as the solid curve in Fig. 7 and the values of the parameters are given in Table III. The definition of the radius of interaction used here is $R = rA_T^{1/3}$. This parameter set gives a reasonable description of the data in both the highly oscillatory forward angle region and the unstructured region observed for angles greater than 80°. A limited search was made for a discrete potential set with $U=220$ MeV, since discrete potential sets differing by 60 MeV were reported in Refs. 16 and 17. The final fit was similar but clearly inferior to the fit for the 159-MeV potential set. The calculation for $U=220$ MeV underpredicted the cross section in the angular region from 50°–80°, and it is not apparent that discrete equivalent potential sets exist at this

TABLE III. Optical model parameters for ^{6}Li + ^{12}C at $E=60$ MeV.

Set	U (MeV)	W_v (MeV) [a]	r_r (fm) [b]	a_r (fm)	r_i (fm) [b]	a_i (fm)	r_c (fm) [b]	β_2 [a]	$\beta_2 R_W$ [a] (fm)
1	159.5	10.73 (8.0)	1.23	0.75	2.42	0.80	2.0	(−0.35)	(−1.94)
2	20.0	9.8 (9.0)	2.17	0.56	2.19	1.06	2.3	(−0.27)	(−1.67)
3	59.6	32.0	1.75	0.74	2.25	0.39	2.42		

[a] The numbers in parentheses were obtained in the coupled-channels analysis.
[b] $R = rA_t^{1/3}$.

higher bombarding energy. More data on different targets would help in clarifying the presence of discrete potential sets at these higher energies.

In ^{16}O elastic scattering analyses the physical size of the projectile is generally accounted for by using the definition $R = r_0(A_T^{1/3} + A_P^{1/3})$ for the potential radius. The parameter r_0 typically has the value 1.2 fm. To find potential sets which contain this larger interaction radius, grid calculations were carried out with the following parameter ranges and step sizes: $U = 20-260$ MeV, $\Delta U = 20$ MeV; $W = 5-50$ MeV, $\Delta W = 5$ MeV; $r_r = 1.2$ fm; $a_r = 0.6-1.2$ fm, $\Delta a_r = 0.2$ fm; $r_i = 1.2-2.7$ fm, $\Delta r_i = 0.3$ fm; $a_i = 0.6-1.2$ fm, $\Delta a_i = 0.2$ fm; $r_c = 1.3$ fm. The χ^2 grids obtained were characterized by shallow and poorly defined minima. Direct searches were done around 31 different minima to find the best potential set with the larger radius definition. The potential set obtained is Set 2 in Table III, and the calculated angular distribution is shown in Fig. 7. The major difference in fitting the data between this extremely shallow parameter set and the set discussed earlier is the continuous oscillation of the calculated cross section as a function of increasing angle. The fit to the data for angles less than 50° is superior to that for parameter set 1; however, the data for angles greater than 80° are not described.

Also shown as Set 3 in Fig. 7 is the calculated cross section using an energy dependent set of potentials determined from fitting $^6Li + ^{12}C$ scattering data taken in the energy range 20–40 MeV.[18] As can be seen, the calculated cross section is larger than the data for all but the most forward angles. This difficulty was noticed by Bindal *et al.*[18] when the 63-MeV data of Ref. 11 was included in the analysis. However, Bindal *et al.*[18] assumed the 63-MeV data to be in error by a factor of 3.5. Since the data reported here agree very well with the data of Ollerhead *et al.*,[11] it is apparent that the energy dependent optical potential parametrization of Ref. 18 cannot be used at the higher energies of this work.

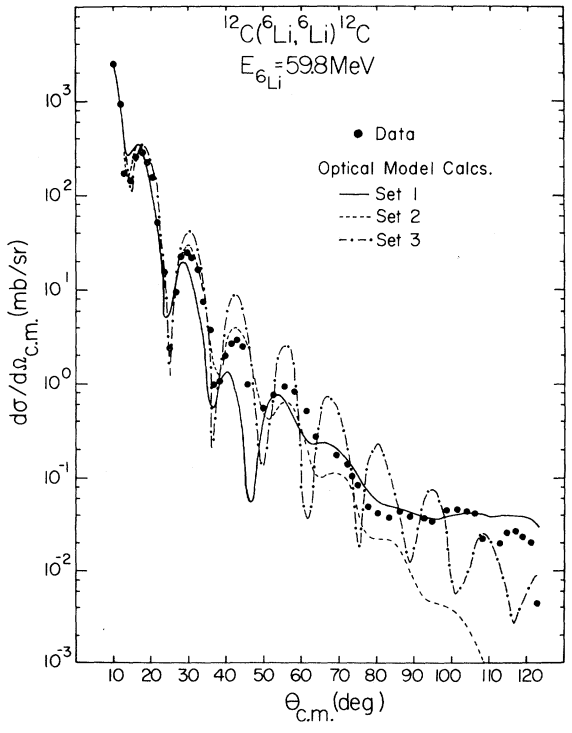

FIG. 7. Optical model calculations for the elastic scattering. The three sets of optical model parameters are given in Table III.

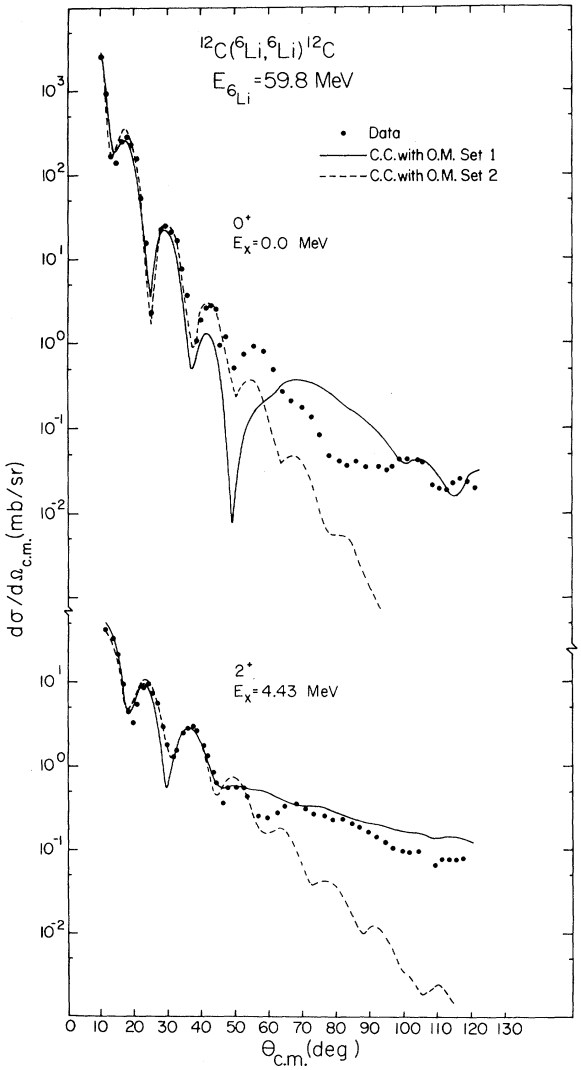

FIG. 8. Results of coupled-channels calculations done with parameter sets given in Table III. The error bars are contained within the data points.

The inelastic scattering to the ^{12}C first excited state was analyzed with the coupled-channels program JUPITOR[19] to study further the two optical parameter sets. The target nucleus was assumed to be axially symmetric. Macroscopic, collective, complex form factors were used in the calculation. In addition, a Legendre expansion of the potentials was used. Fifty partial waves were sufficient for the calculations. Since the explicit inclusion of the scattering to the strongly excited 2^+ state should lead to a decrease in the imaginary potential, only the quadrupole deformation β_2 and the imaginary potential were varied until the best fit to the 2^+ data was found. The calculated inelastic scattering cross sections are shown in Fig. 8 along with the data. In the calculation shown for optical potential parameter set 1, the imaginary potential was reduced from 10.73 to 8.0 MeV, the deformation parameter had the value $\beta_2 = -0.350$, and the deformation length was $\beta_2 R_w = 1.94$ fm. For parameter set 2, W_v, was reduced to 9.0 MeV from 9.8 MeV, the deformation value was $\beta_2 = -0.270$, and the deformation length was $\beta_2 R_w = 1.67$ fm. The fits to the data for optical parameter set 1 are quite reasonable except for the elastic scattering for angles greater than 45°. Parameter variations of ±10% around the values given in Table III did not show any real improvement in the fit. This deficiency in the calculation is not surprising in view of the large number of assumptions made in these calculations. For optical parameter set 2, the calculated inelastic cross section has the same characteristic as the elastic cross section, i.e., it provides a good fit to the forward angle data but underpredicts the data for angles greater than 55°. The values of the deformation lengths extracted are at the high end of the range of values, 1.3–1.8, of deformation lengths which have been reported for (p, p') scattering and for lower energy ^{6}Li scattering studies.[17,18,20] In summary, this analysis of the 60-MeV elastic and inelastic scattering data shows that the optical model and coupled-channels techniques are able to describe the ^{6}Li + ^{12}C data even though ^{6}Li is a relatively complex projectile.

B. Three particle transfer reactions

In previous comparison studies[2,3] of the (^{6}Li, t) and (^{6}Li, ^{3}He) reactions on self-conjugate nuclei, it has been possible to identify mirror states from the relative intensity of the states populated and the shapes of the measured angular distributions. The identification of analog states with this technique has been extremely successful, encountering difficulty only with weakly excited states.[3] As can be seen in Fig. 2, strongly excited states, which are obvious analog pairs, are at excitation energies of 10.50-10.73, 12.88-13.15, and 15.05-15.49 MeV in ^{15}O-^{15}N, respectively. For the weaker states assignment of analog pairs is complicated by the experimental energy resolution of 200 keV, since a given peak can contain contributions from several states and the major contributor cannot be determined.

In addition, it is possible that even the strongly excited states are due to the enhanced population of several states in that region of excitation. The higher resolution spectrum in Fig. 1 shows the peaks at excitation energies of 10.45, 12.84, and 15.05 MeV in ^{15}O contain contributions from single states, at least within the 45-keV experimental energy resolution. It is assumed in the remainder of this work that the three strong peaks in the ^{15}O-^{15}N spectra are due to the excitation of only one state. In addition, the energies quoted for the states in ^{15}O are those obtained from the magnetic spectrograph data. A study of the ^{12}C(^{6}Li, ^{3}He-t) reactions at a bombarding energy of 24 MeV[21] has assigned analog pairs which correspond, in the present work, to ^{15}O-^{15}N states at 5.24-5.27, 6.92-7.24, 7.29-7.61, and 8.33-8.59 MeV. The peaks at 5.24 MeV in ^{15}O and 5.27 MeV in ^{15}N contain contributions from two states. The angular distributions for the seven pairs of analog states are shown in Fig. 3.

In the reactions ^{12}C(^{10}B, ^{7}Li-^{7}Be) done at an incident energy of 100 MeV, Nagatani *et al.*[14] identified analog pairs in ^{15}O-^{15}N at excitation energies of 9.64-9.87, 10.47-10.78, 12.89-13.15, 15.36-15.72, 15.88-16.26, and 17.13-17.83 MeV. The present work confirms the assignment of analog pairs at 10.47-10.78, 12.89-13.15, and 15.36-15.72 MeV except that the (^{6}Li, t) reaction yields an energy of 15.05 MeV for the state in ^{15}O. The excitation energy found in the present work is in good agreement with the ^{12}C(^{12}C, ^{9}Be)^{15}O measurement of Scott *et al.*,[22] who found a strongly excited state at 15.08 MeV. The higher resolution (^{6}Li, t) spectrum shown in Fig. 1 indicates that the peaks in the ^{10}B-induced reactions at 9.64, 15.88, and 17.13 MeV in ^{15}O contain contributions from two or more states making the identification of analog pairs extremely uncertain for these groups of states.

A detailed study of the ^{12}C(^{7}Li, α)^{15}N reaction by Tserruya, Rosner, and Bethge[23] at a bombarding energy of 35 MeV indicates that the (^{7}Li, α) reaction proceeds by a direct triton stripping mechanism and selectively populates three-particle–four-hole states. Studies of the ^{16}O(^{6}Li, ^{3}He-t)^{19}F reaction[2,4] also conclude that these reactions are direct three-particle stripping reactions. Both the (^{7}Li, α) and (^{6}Li, ^{3}He) reactions should populate the same types of states, but since they have a differ-

ence in angular momentum mismatch of about $3\hbar$, with the (^{7}Li, α) being the better matched reaction ($\sim 2\hbar$), the relative population of states by the two reactions should also give an indication of the spins of the states populated. In the ^{12}C(^{7}Li, α)^{15}N reaction,[23] four strongly excited states occur at excitation energies of 10.70, 12.56, 13.17, and 15.37 MeV, while in the ^{12}C(^{6}Li, ^{3}He) reaction, strongly excited states occur at 10.73, 13.15, and 15.49 MeV with the state at 12.64 MeV having only one-fifth the intensity of the 13.15-MeV state. Angular momentum mismatch arguments would suggest that the spin of the 12.64-MeV state is less than that of either the 10.73- or 13.15-MeV states. Also, if the state seen at 15.37 MeV in the (^{7}Li, α) reaction is associated with the 15.49-MeV state in the present work, then intensity arguments suggest the 15.49-MeV state has a higher spin than either the 10.73- or 13.15-MeV states. Clearly, though, effects other than just angular momentum mismatch are present. In the (^{7}Li, α) reaction, the ratio of cross sections for the 9.16 MeV ($J = \frac{5}{2}$) and 7.57 MeV ($J = \frac{7}{2}$) states is 2.74/0.15, while in the present work it is 0.120/0.106.

In an attempt to gain some knowledge of the spins of the analog states populated, exact finite range DWBA calculations assuming the transfer of a ^{3}He cluster have been performed with the code MERCURY[24] for the reaction ^{12}C(^{6}Li, t)^{15}O. The bound state form factor for the ^{6}Li $\rightarrow$ ^{3}He + t system was generated with a Woods-Saxon-plus-Coulomb potential having the geometrical parameters $r_0 = r_{0c} = 1.73$ fm and diffuseness $a = 0.45$ fm. These parameters are from an optical model analysis of ^{3}He-^{3}He elastic scattering done by Thompson and Tang.[25] The bound state potential well depth was 82 MeV and it was assumed that the two clusters are in a relative $2s$ state. This latter assumption should make the (^{6}Li, ^{3}He) reaction more distinctive than the (^{7}Li, α) reaction since in the (^{6}Li, ^{3}He) reaction only one L transfer occurs, whereas in the (^{7}Li, α) reaction three L transfers occur except for transitions to $\frac{1}{2}^+$ states. For the ^{12}C + ^{3}He or t bound state system, the potential parameters of Ref. 2 ($r_0 = r_{0c} = 2.0$ fm and $a = 0.65$ fm) were used and the potential well depths were varied to give the correct $t/^3$He binding energy $B = [15.79 + Q(^6\text{Li}, ^3\text{He}\text{-}t)]$ MeV. For the unbound states, a binding energy of -0.5 MeV was assumed. Optical model parameter set 1 in Table III was used for ^{6}Li + ^{12}C in the DWBA calculations. This choice of parameters was based on the success of DWBA calculations in describing the angular distributions of Li-induced single nucleon transfer reactions in the $1p$ shell,[17] the $2s$-$1d$ shell,[26] and in the f-p shell[27] at bombarding energies of 34–36 MeV. The t + ^{15}O and ^{3}He + ^{15}N optical model parameters used were taken from a study of the (p, t) and (p, ^{3}He) reactions on ^{14}N, ^{15}N, and ^{18}O by Pignanelli *et al.*[28] The values of the potential parameters were $U = 162.9$

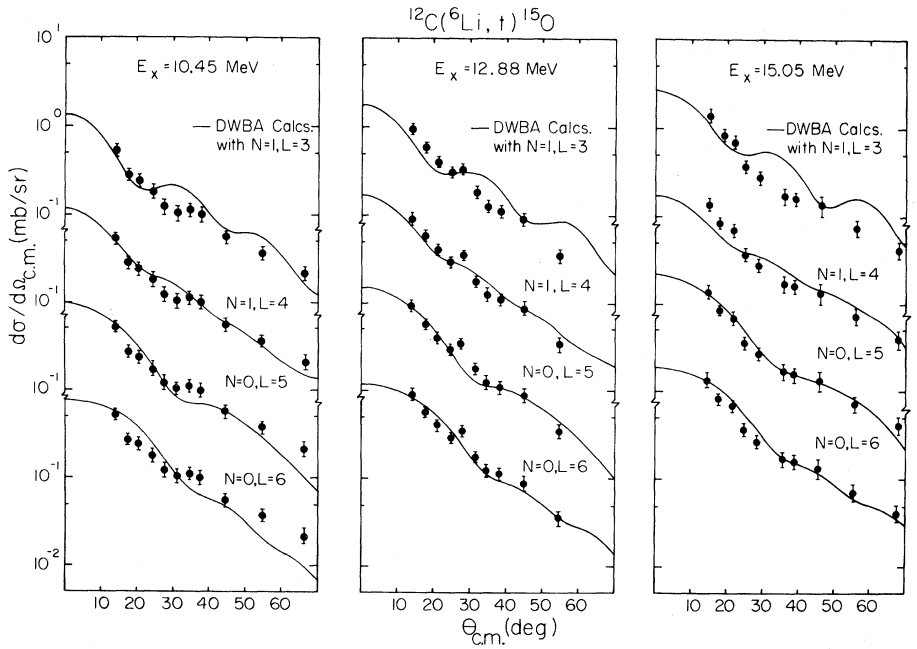

FIG. 9. DWBA calculations for the reaction ^{12}C(^{6}Li, t)^{15}O to the most strongly excited states in ^{15}O. The solid curves are the result of calculations with bound state configurations for the system ^{12}C + ^{3}He having the N and L values shown.

MeV, $r_r=1.14$ fm, $a_r=0.50$ fm, $W_v=11.84$ MeV, $r_i=1.82$ fm, $a_i=0.56$ fm, and $r_c=1.25$ fm. In addition, assumptions as to the possible L transfers must be made to carry out the calculations.

Scott *et al.*[22] have suggested from the intensity of the states populated in the ^{12}C(^{12}C, ^{9}Be) reaction that the state at 15.05 MeV in ^{15}O is the $\frac{13}{2}^+$ member of the $(d_{5/2})^3$ configuration. If it is assumed that the level ordering for the $(d_{5/2})^3$ configuration resembles the ground state rotational band in $A=19$ ($\frac{1}{2}^+, \frac{5}{2}^+, \frac{3}{2}^+, \frac{9}{2}^+, \frac{13}{2}^+, \frac{7}{2}^+, \frac{11}{2}^+$), then the $\frac{9}{2}^+$ state would lie below the 15.05-MeV state. The state at 10.45 MeV is assumed to be the $\frac{9}{2}^+$ member of the $(d_{5/2})^3$ configuration since the strongest state populated in the ^{13}C(α, d)^{15}N reaction[29] occurs at 13.03 MeV and has been assigned the configuration $[(d_{5/2})^2 p_{1/2}]_{11/2^-}$ on the basis of systematics. In the present analysis, it is assumed that the analog state at 12.84 MeV in ^{15}O has the configuration $[(d_{5/2})^2 p_{1/2}]_{11/2^-}$. In the ^{13}C($\alpha, d$)^{15}N work, a state at 11.95 MeV, populated with less than one-half the intensity of the 13.03-MeV state at forward angles, was assigned as the $[(d_{5/2})^2 p_{1/2}]_{9/2^-}$ state. This assignment is probably in error since this state is not strongly populated in either the (^{6}Li, ^{3}He) or (^{10}B, ^{7}Be) reactions and it should be.

From these considerations, the ^{12}C + ^{3}He quantum numbers for the clusters in the bound states were assumed to have $2N+L=5$ or 6. The calculations with $N=1$, $L=3$, $N=1$, $L=4$, $N=0$, $L=5$ and $N=0$, $L=6$ are shown in Fig. 9 for the 10.45-, 12.84-, and 15.05-MeV states. The latter two states are unbound. Within the limits of the assumptions made in the calculations, the transferred L values which provide the best fit to the data are $L=4$ or 5 for the 10.45-MeV state, $L=4, 5$, or 6 for the 12.88-MeV state, and $L=5$ or 6 for the 15.05-MeV state. Calculations were also done for the low-lying analog pairs but because the small cross sections limited the angular range over which data could be extracted, no conclusion could be reached as to how well the calculations were able to fit the data for states of known spins.

From the identification of analog pairs corresponding structure assignments in ^{15}N can be made on the basis of the ^{15}O results. In ^{15}N, the states at 10.73 and 15.49 MeV are the $\frac{11}{2}^+$ and $\frac{13}{2}^+$ members of the $(d_{5/2})^3$ configuration and the 13.15-MeV state is the $\frac{11}{2}^-$ state of configuration $(d_{5/2})^2 p_{1/2}$. Comparisons with the $A=19$ system suggest the state at 12.56 MeV, strongly excited in the ^{12}C(^{7}Li, α) reaction, but not in the ^{12}C(^{6}Li, ^{3}He) reaction, is the $\frac{3}{2}^+$ member of the $(d_{5/2})^3$ configuration. Cluster model calculations[30] done for the $A=15$ system assuming ^{15}N = ^{12}C + t agree well with these assignments for ^{15}N and in addition predict that the states with configurations $[(d_{5/2})^2 p_{1/2}]_{9/2^-}$ and $[(d_{5/2})^3]_{11/2^+}$ lie at excitation energies 9 MeV above the 15.49-MeV state. Consequently, the present study would not have observed either of these states.

V. CONCLUSIONS

The elastic scattering of ^{6}Li by ^{12}C at 60 MeV has been reasonably well described with optical model parameters that also fit data taken in the energy range 28–36 MeV. A coupled-channels analysis of the inelastic scattering data yields deformation lengths which agree with values extracted from the (p, p') studies.

From the intensity of the states populated and the shapes of angular distributions, analog pairs in ^{15}O-^{15}N have been identified at excitation energies of 10.45-10.73, 12.84-13.15, and 15.05-15.49 MeV.

Exact finite range DWBA calculations indicate the possiblity that transferred angular momenta can be extracted from the shapes of the angular distributions of the (^{6}Li, ^{3}He-t) reactions when sufficient data exist. While much more data need to be taken on the three particle transfer reactions at the higher energy used in this work to test the reliability of extracting L transfers from the (^{6}Li, t) and (^{6}Li, ^{3}He) reactions, the present results are encouraging.

ACKNOWLEDGMENTS

This experiment was made possible by the interested cooperation of the ORIC staff in developing the lithium beam. We wish especially to thank M. L. Mallory, E. D. Hudson, and F. Irwin for their work on the ion source. We also wish to thank Leigh Harwood for his aid with some of the calculations. One of the authors (KWK) also acknowledges support from the Oak Ridge Associated Universities, Inc.

---

†Deceased 8 April 1974. The other authors of this work express gratitude for having had the opportunity to have Hans Bingham as a colleague.

*Work supported by Union Carbide under contract with the U.S. Atomic Energy Commission.

‡Work supported in part by the National Science Foundation under Grants Nos. NSF-GP-25974, NSF-GU-2612, NSF-GP-41834X, and NSF-GJ-367.

[1] H. G. Bingham, H. T. Fortune, J. D. Garrett, and R. Middleton, Phys. Rev. Lett. 26, 1448 (1971).

[2]J. D. Garrett, H. G. Bingham, H. T. Fortune, and R. Middleton, Phys. Rev. C 5, 682 (1972).
[3]H. G. Bingham, H. T. Fortune, J. D. Garrett, and R. Middleton, Phys. Rev. C 7, 57 (1973); C. H. Holbrow, H. G. Bingham, R. Middleton, and J. D. Garrett, *ibid.* 9, 902 (1974).
[4]A. D. Panagiotou and H. E. Gove, Nucl. Phys. A196, 145 (1972).
[5]E. D. Hudson, M. L. Mallory, and S. W. Mosko, IEEE Trans. Nucl. Sci. NS-18, 113 (1971).
[6]C. D. Goodman, C. A. Ludemann, D. C. Hensley, R. Kunz, and E. W. Anderson, IEEE Trans. Nucl. Sci. NS-18, 323 (1971).
[7]D. C. Hensley and C. D. Goodman, IEEE Trans. Nucl. Sci. NS-18, 312 (1971).
[8]J. Borggreen, B. Elbek, and L. P. Nielson, Nucl. Instrum. Methods 24, 1 (1963).
[9]J. B. Ball, IEEE Trans. Nucl. Sci. NS-13, 340 (1966).
[10]J. E. Draper, Rev. Sci. Instrum. 37, 969 (1966).
[11]R. W. Ollerhead, C. Chasman, and D. A. Bromley, Phys. Rev. 134, B74 (1964).
[12]F. Ajzenberg-Selove, Nucl. Phys. A152, 1 (1970).
[13]F. Ajzenberg-Selove, Nucl. Phys. A166, 1 (1971).
[14]K. Nagatani, D. H. Youngblood, R. Kenefick, J. Bronson, Phys. Rev. Lett. 31, 250 (1973).
[15]F. G. Perey, Phys. Rev. 131, 745 (1963); A. W. Obst, Florida State University Report JIB (unpublished).
[16]G. Bassani, N. Saunier, B. M. Traore, J. Raynal, A. Foti, and G. Pappalardo, Nucl. Phys. A189, 353 (1972).
[17]P. Schumacher, N. Ueta, H. H. Duhm, K. I. Kubo, and W. J. Klages, Nucl. Phys. A212, 573 (1973).
[18]P. K. Bindal, K. Nagatani, M. J. Schneider, and P. D. Bond, Phys. Rev. C 9, 2154 (1974).
[19]T. Tamura, Rev. Mod. Phys. 37, 679 (1965); Oak Ridge National Laboratory Report No. 4152 (unpublished).
[20]G. R. Satchler, Nucl. Phys. 100, 497 (1967).
[21]C. H. Holbrow, H. G. Bingham, and J. D. Garrett, Bull. Am. Phys. Soc. 17, 465 (1972).
[22]D. K. Scott, P. N. Hudson, P. S. Fisher, C. U. Cardinal, N. Anyas-Weiss, A. D. Panagiotou, P. J. Ellis, and B. Buck, Phys. Rev. Lett. 28, 1659 (1972).
[23]I. Tserruya, B. Rosner, and K. Bethge, Nucl. Phys. A213, 22 (1973).
[24]L. A. Charlton, Phys. Rev. C 8, 146 (1973); L. A. Charlton and D. Robson, Florida State University Technical Report No. 5, MERCURY (unpublished).
[25]D. R. Thompson and Y. C. Tang, Phys. Rev. 159, 806 (1967).
[26]G. E. Moore, K. W. Kemper, and L. A. Charlton, Phys. Rev. (to be published).
[27]G. M. Hudson, K. W. Kemper, G. E. Moore, and M. E. Williams (unpublished).
[28]M. Pignanelli, S. Micheletti, I. Iori, P. Guazzoni, F. G. Resmini, and J. L. Escudiê, Phys. Rev. C 10, 445 (1974).
[29]C. C. Lu, M. S. Zisman, and B. G. Harvey, Phys. Rev. 186, 1086 (1969).
[30]B. Buck, C. B. Dover, and J. P. Vary, Bull. Am. Phys. Soc. 18, 1414 (1973).